

Interpretation of the giant magnetoresistance effect in Co/Cu(100) multilayers with the quantum model of giant magnetoresistance

S.K.J. Lenczowski

Eindhoven University of Technology, Department of Physics, 5600 MB Eindhoven, The Netherlands

M.A.M. Gijs and J.B. Giesbers

Philips Research Laboratories, Professor Holstlaan 4, 5656 AA Eindhoven, The Netherlands

R.J.M. van de Veerdonk and W.J.M. de Jonge

Eindhoven University of Technology, Department of Physics, 5600 MB Eindhoven, The Netherlands

(Received 25 April 1994)

We have measured the magnetoresistance of high-vacuum-sputtered Co/Cu(100) multilayers grown on Cu buffer layers. The magnetoresistance in the first antiferromagnetic- (AF-) coupling peak is very sensitive to the buffer layer thickness. We find a linear dependence between the actual measured magnetoresistance and the fraction of AF coupling, as determined by magnetization measurements. We compare our Co/Cu(100) magnetoresistance data at 4 K of completely antiparallel-aligned multilayers with the quantum model of giant magnetoresistance of Levy, Zhang, and Fert. This reveals evidence for strong spin-dependent interface scattering, whereas the spin dependence of the bulk scattering in Co is small.

I. INTRODUCTION

The giant magnetoresistance (MR) effect in magnetic multilayers has been the subject of numerous studies in recent years (see, for instance, Refs. 1–3 and references therein). On the basis of the giant MR effect, there is a spin dependence of the electron scattering processes, but whether this spin-dependent scattering takes place within the interior of the magnetic layers or at the interfaces between magnetic and nonmagnetic materials still remains a matter of dispute. Since Camley and Barnaś originally introduced their semiclassical MR model based on the spin-dependent Boltzmann equation,⁴ it has been widely applied in modified forms to several multilayer and spin-valve systems.^{5–10} The semiclassical approach gives good qualitative results and, moreover, a quantitative agreement with the experimental data can also be obtained in terms of model parameters.¹¹ An essential drawback, however, is the different treatment of the bulk and interface contributions to the resistivity. Levy, Zhang, and Fert on the other hand developed a quantum model of the MR,¹² which describes both bulk and interface scattering on equal footing. This model was used to explain the giant MR of the Fe/Cr system,¹³ which is a good model system, since due to the large antiferromagnetic- (AF-) coupling strength, full antiparallel alignments at zero applied field can be realized relatively easily up to Cr spacer layer thicknesses of 2.8 nm, corresponding to the second AF-coupling maximum. For the Fe/Cr case it was concluded that the spin-dependent scattering processes are primarily of interfacial nature. In the case of Co/Cu multilayers such a comparison is more difficult, because the much weaker AF-coupling strength easily causes an imperfect antiparallel alignment already in the first AF-

coupling peak and certainly in the second peak, thereby reducing the measured MR value and leading to data inappropriate for comparison with the model.

In this paper we present MR measurements on Co/Cu(100) multilayers grown by sputtering techniques. This system is known to exhibit large MR values and can be grown coherently in a rather easy way.¹⁴ The influence of the Cu buffer layer thickness t_b , deposited prior to the multilayer to obtain a well-defined (100) growth, on the fraction of AF coupling is discussed. We find that t_b has a large influence on that fraction, especially for Cu spacer layer thicknesses corresponding to the first AF-coupling peak. Measured MR values are directly proportional to the AF-coupled fraction in the multilayers. Extrapolating our MR data to full antiparallel alignment, we can make a reliable comparison of the MR of Co/Cu(100) at 4 K with the quantum model of Levy, Zhang, and Fert.¹²

II. SAMPLE PREPARATION AND CHARACTERIZATION

The multilayer samples were grown by high-vacuum magnetron sputtering. The base pressure of the system prior to deposition was 4×10^{-7} Torr and the Ar pressure during the sputtering was 7×10^{-3} Torr. The samples were deposited at a rate of 4 Å/s onto 4×12 mm² Si(100) substrates held at room temperature. Before sputtering, the samples were *ex situ* cleaned by a HF dip and *in situ* by a 30-min glow-discharge treatment. In order to obtain a highly face centered cubic (fcc) (100)-oriented texture, we used Cu buffer layers with thicknesses t_b of 200 and 300 Å. For values of t_b below 200 Å we get a mixed

(111)-(100) growth. After deposition of the multilayers, they were covered with a 50-Å Au protection layer. The (100) orientation was checked by x-ray-diffraction (XRD) measurements using Cu $K\alpha$ radiation. Figure 1 shows a typical high-angle XRD pattern for the superlattice $100 \times (16 \text{ \AA} \text{ Co} + 10.5 \text{ \AA} \text{ Cu})$ grown on top of a 200-Å Cu buffer layer. We observe the main Co/Cu(200) Bragg reflection with several multilayer satellite peaks, very similar to earlier results of Coehoorn *et al.*¹⁵ There is almost no intensity of Co/Cu(111) reflections present. From the full width at half maximum (FWHM) of the Co/Cu(200) reflection, which is 0.39° , we deduce a perpendicular crystal coherence length of about 240 Å. This value is nearly the same for all our (100)-oriented multilayers. The FWHM of the rocking curves about the (200) maximum (not shown) varied between 1.5° and 2.0° , indicating the good texture of the crystallites.

III. MAGNETORESISTANCE AND MAGNETIZATION MEASUREMENTS

Typical magnetoresistance curves for two samples grown on a 200-Å Cu buffer layer and with Cu spacer layer thicknesses t_{Cu} of 10.5 Å and 20 Å are shown in Figs. 2(a) and 2(b), respectively. We define MR as $(R_{\text{max}} - R_{\text{sat}})/R_{\text{sat}}$, with R_{max} the maximum resistance around zero field and R_{sat} the value at saturation. High MR values at room temperature are found of 48% (83% at 4 K) for the multilayer with $t_{\text{Cu}} = 10.5 \text{ \AA}$ and 40% (75% at 4 K) for the multilayer with $t_{\text{Cu}} = 20 \text{ \AA}$. The characteristic form of these curves is a consequence of the fact that the magnetic field was applied along a hard magnetization axis, as we will discuss further in more detail in relation to the magnetization experiments. Fig-

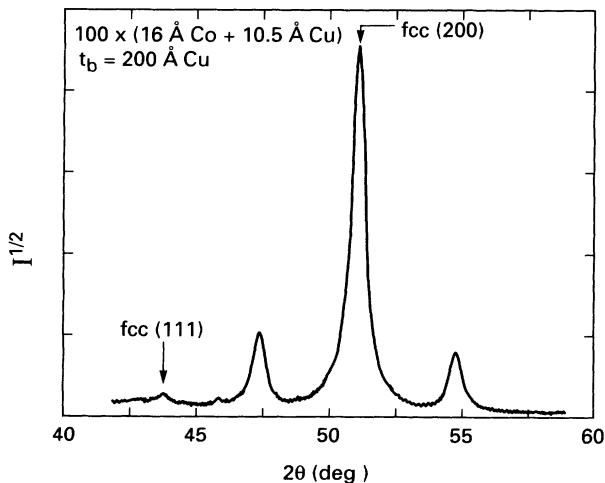


FIG. 1. High-angle x-ray-diffraction pattern of a $100 \times (16 \text{ \AA} \text{ Co} + 10.5 \text{ \AA} \text{ Cu})$ multilayer grown on top of a 200-Å Cu buffer layer.

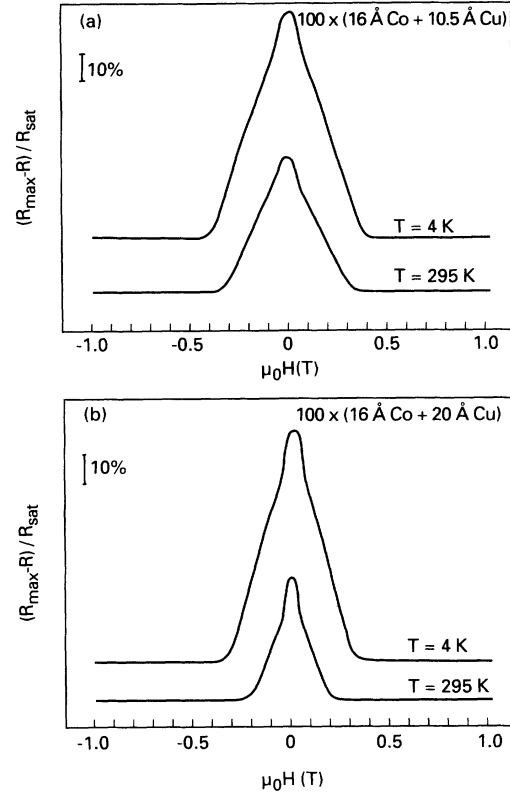


FIG. 2. Magnetoresistance curves at room temperature and 4 K for (100)-oriented samples (a) $100 \times (16 \text{ \AA} \text{ Co} + 10.5 \text{ \AA} \text{ Cu})$ and (b) $100 \times (16 \text{ \AA} \text{ Co} + 20 \text{ \AA} \text{ Cu})$ grown on a 200-Å Cu buffer layer. The magnetic field was along a cubic hard magnetization axis.

ure 3 depicts the magnetoresistance at room temperature as a function of t_{Cu} for a series of multilayers on 200- and 300-Å Cu buffer layers. One can observe an oscillatory behavior with a period of about 10 Å, which can be associated with maxima in the AF interlayer exchange coupling in this system (see, for instance, Refs. 15–18). Note, however, that the first AF peak around $t_{\text{Cu}} = 10 \text{ \AA}$ is nearly absent for multilayers grown on a 300-Å-thick buffer layer. Similar results were found by Giron *et al.*¹⁹ and they attributed this phenomenon to the roughness of the multilayers and pinholes causing effective ferromagnetic coupling. Because of the relative importance of the roughness compared to t_{Cu} , this effect is more important for the first than for the second AF peak. Apparently, there is a critical maximum value for the buffer layer thickness, since for Fe/Cr multilayers, interface roughness has also been found to increase cumulatively with increasing number of layers.²⁰ To support this idea, we show in Figs. 4(a) and 4(b) atomic force microscopy (AFM) pictures on the surface roughness of samples consisting of a limited number (four) of $(16 \text{ \AA} \text{ Co} + 10 \text{ \AA} \text{ Cu})$ bilayers grown on a 200- and 300-Å-thick Cu buffer layer, respectively. We find that the sample on a 200-Å Cu buffer layer [Fig. 4(a)], with a mean roughness of about 5 Å, is substantially smoother

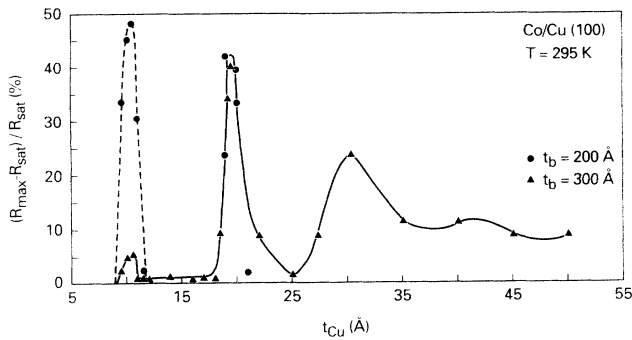


FIG. 3. Dependence of the MR ratio at room temperature on the Cu spacer layer thickness t_{Cu} for (100)-oriented $100 \times (16 \text{ \AA} \text{ Co} + t_{\text{Cu}} \text{ \AA} \text{ Cu})$ multilayers grown on (O) 200-Å and (Δ) 300-Å Cu buffer layers. The solid and dashed lines are guides to the eye.

than the sample on a 300-Å Cu buffer layer, with a mean roughness of about 12 Å [Fig. 4(b)]. A noticeable difference in surface roughness, although smaller, could already be observed in single Cu layers of 200 and 300 Å. So we indeed have evidence that the initially larger surface roughness of a 300-Å Cu base layer leads to relatively rougher multilayers grown on top.

The large difference in MR value found in the first AF coupling peak for the two series of multilayers grown on a 200-

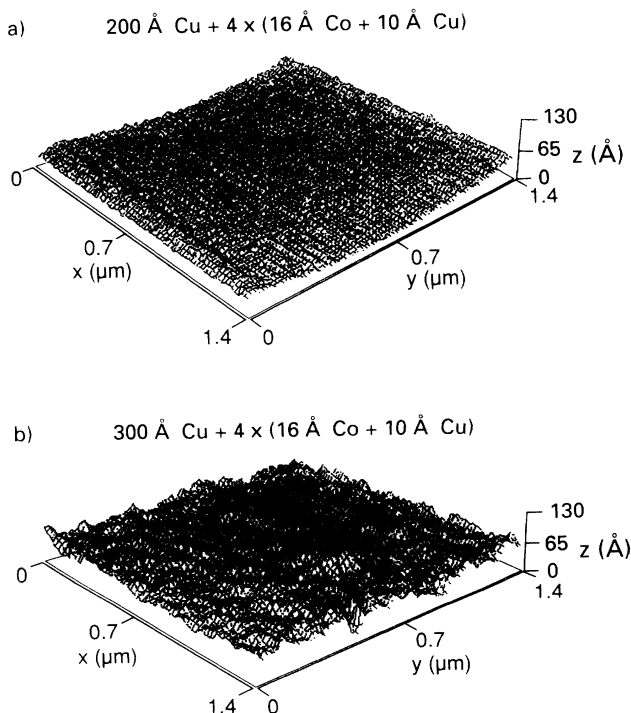


FIG. 4. Atomic force microscopy (AFM) pictures of $4 \times (16 \text{ \AA} \text{ Co} + 10 \text{ \AA} \text{ Cu})$ samples grown on (a) 200-Å Cu and (b) 300-Å Cu. The x and y directions are in the plane of the layers, whereas in the z direction the surface roughness is shown. For the sample grown on a 200-Å Cu buffer layer the typical roughness is about 5 Å and for the sample on a 300-Å Cu buffer layer it is about 12 Å.

and 300-Å thick Cu buffer layer cannot be, as mentioned above, a structural effect in the sense that growth orientation or multilayer periods differ largely for both series, since no evidence for that was found in the XRD data. Shunting effects in the buffer and protection layers can also be excluded considering the magnitude of the MR difference. In order to investigate whether a difference in electronic properties may account for the difference in MR values, such as for instance the ratio $\alpha = \lambda_{\uparrow} / \lambda_{\downarrow}$, where λ_{\uparrow} and λ_{\downarrow} are the elastic scattering lengths for spin-up and spin-down electrons, respectively, we measured the temperature dependence of the MR for identical samples grown on a different buffer layer thickness (both samples correspond to the maximum of the first AF-coupling peak). In that case one would expect a much smaller temperature dependence for the series on $t_b = 300 \text{ \AA}$ exhibiting the low MR values. Figure 5 shows the normalized temperature dependence of the MR for both samples. We obtain an identical behavior, where the MR reaches a value of 83% at 4 K for the multilayer grown on a 200-Å Cu buffer layer and only 8.6% for the multilayer on a 300-Å Cu buffer layer. This identical temperature dependence again suggests that electronic spin-dependent scattering processes are not essentially different and that it is just the fraction of AF coupling that determines here the actual value of the MR, similar to the case of (111)-oriented²¹ and mixed (100)-(110)-oriented Co/Cu superlattices grown on a variety of buffer layers and under various conditions.²²

We determined the AF-coupling behavior by means of magnetization measurements using a vibrating sample magnetometer (VSM). The magnetic field H was always in the plane of the layers. All our samples had a cubic fourfold in-plane anisotropy with the easy magnetization

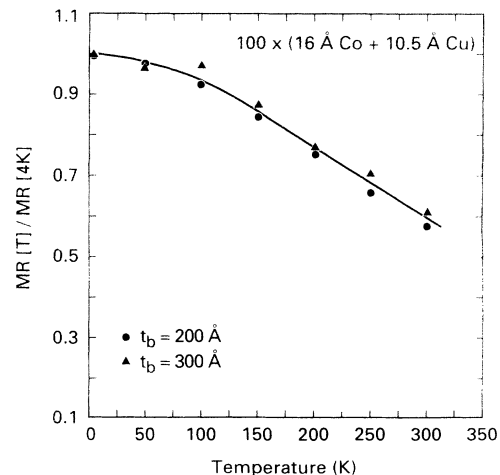


FIG. 5. Temperature dependence of the MR for (100)-oriented $100 \times (16 \text{ \AA} \text{ Co} + 10.5 \text{ \AA} \text{ Cu})$ multilayers grown on a (O) 200-Å and (Δ) 300-Å Cu buffer layer. Both samples correspond to the maximum of the first AF-coupling peak. For the sample on a 200-Å Cu buffer layer, the MR value at 4 K reaches 83%; for the sample on a 300-Å Cu buffer layer the MR is only 8.6% at 4 K.

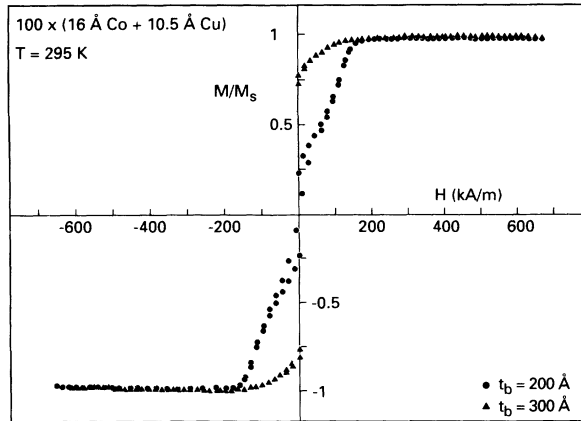


FIG. 6. Magnetic hysteresis loops of (100)-oriented $100 \times (16 \text{ \AA} \text{ Co} + 10.5 \text{ \AA} \text{ Cu})$ multilayers grown on a (O) 200-Å and (Δ) 300-Å Cu buffer layer. Both samples correspond to the maximum of the first AF-coupling peak. The magnetic field H is applied parallel to the easy [011] direction.

axis along the crystallographic [011] axis and the hard axis for magnetization along the crystallographic [001] axis. When H is applied parallel to the easy [011] direction, the fraction of AF coupling is defined by $1 - M_r/M_s$, with M_r the remanent magnetization at zero field and M_s the saturation magnetization. Figure 6 displays the magnetic hysteresis loops at room temperature of the samples with $t_{\text{Cu}} = 10.5 \text{ \AA}$ on a 200- and 300-Å Cu buffer layer, corresponding to the first AF-coupling maximum. The sample on the 300-Å Cu buffer layer clearly shows a large M_r , indicative for a large ferromagnetic coupling fraction, whereas the situation for the other sample is just opposite.

In order to extract values for the AF-coupling strength J_{AF} and the cubic magnetocrystalline anisotropy constant K_1 from the magnetization measurements, we used the expression

$$J_{\text{AF}} = \frac{(H_s - H^*) M_s t_{\text{Co}}}{4}, \quad (1)$$

which has been derived from absolute minimum energy calculations.^{23,24} Here, H_s denotes the saturation field along the hard [001] direction and $H^* = 2 K_1/\mu_0 M_s$.

Determination of H^* from the saturation field of ferromagnetically coupled samples with adjacent t_{Cu} yielded an anisotropy constant $K_1 = -8 \times 10^4 \text{ J/m}^3$, independent of t_{Cu} . This value was confirmed by ferromagnetic resonance measurements. The remanent magnetization for those samples was close to the expected value of $\frac{1}{2}\sqrt{2} M_s$, assuming coherent rotation from the [001] hard axis at saturation to the [011] easy axis at zero field. With the use of Eq. (1) we deduce a maximum coupling strength at room temperature in the first AF peak of J_{AF} (first peak) = 0.15 mJ/m^2 and for the second AF peak J_{AF} (second peak) = 0.068 mJ/m^2 . The value of J_{AF} in the first AF-coupling peak is half the value reported by Coehoorn *et al.*,¹⁵ but in their analysis they neglected the in-plane anisotropy, although its influence seems to be too small to explain the total difference.²⁵ The decay in coupling strength from the first to the second AF peak is of similar magnitude as found for molecular-beam-epitaxy- (MBE-) grown wedge-shaped Co/Cu(100) samples,¹⁸ but our absolute values are less by a factor 2.5.

In Fig. 7(a) we plot for all our samples with t_{Cu} around 10 \AA (samples in the first AF-coupling peak) the MR versus $(1 - M_r/M_s)$. The linear relationship between the MR ratio and the fraction AF coupling allows extrapolation to full antiparallel alignment. Doing so yields for the first AF-coupling peak a maximum MR value of 65% at room temperature (108% at 4 K), which is about the same number as found by Parkin *et al.* for Co/Cu(111) multilayers.²⁶ For the second AF-coupling peak, with $t_{\text{Cu}} \simeq 20 \text{ \AA}$, we find that the MR values are much less sensitive to the thickness of the Cu buffer layer, because the second AF-coupling peak is somewhat broader and the thicker Cu spacer layer prevents the formation of pinholes. This has already been illustrated in Fig. 3, where both samples on a 200- and 300-Å Cu buffer layer exhibit large MR values up to 42%, for t_{Cu} ranging from 18 to 22 Å. In the way described above, we again find a linear dependence of the MR on the fraction of AF coupling [see Fig. 7(b)] and an extrapolated MR value of 46% at room temperature (87% at 4 K) in the limiting case of complete antiparallel alignment.

IV. COMPARISON WITH THE QUANTUM MODEL OF MAGNETORESISTANCE

In this section we will first briefly outline the quantum model of MR of Levy, Zhang, and Fert.¹² In their approach a local in-plane conductivity σ is dependent on

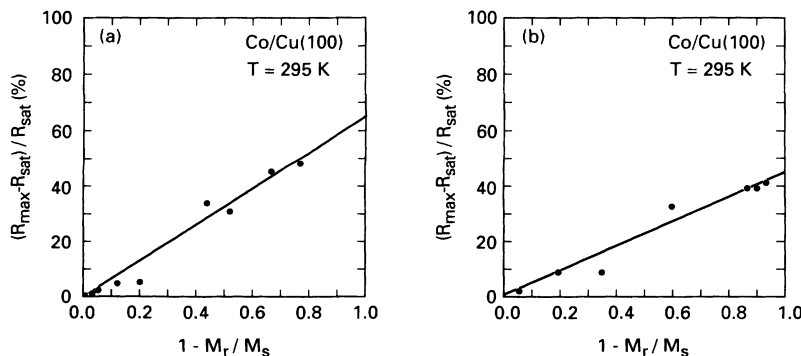


FIG. 7. Room temperature magnetoresistance versus $(1 - M_r/M_s)$ for (100)-oriented $100 \times (16 \text{ \AA} \text{ Co} + t_{\text{Cu}} \text{ \AA} \text{ Cu})$ multilayers with (a) t_{Cu} around the first AF-coupling peak and (b) t_{Cu} around the second AF-coupling peak.

the coordinate z perpendicular to the multilayer planes (lattice planes). An essential difference with the semiclassical model is the representation of the electron by a wave packet having (spin-dependent) scattering probabilities at Co/Cu interfaces or bulk lattice planes. The expressions used in our calculations are summarized below. One should note that Eqs. (2)–(4) are only valid when the magnetizations of the magnetic layers are either parallel or antiparallel:

$$\sigma(z) = \frac{ne^2}{2m} \sum_{\sigma} \frac{\hbar}{E^{\sigma}(z)}, \quad (2)$$

with

$$E^{\sigma}(z) = \frac{\hbar^2 k_F}{m\lambda^{\sigma}} \left\{ \sum_i \operatorname{Re} \Delta_i^{\sigma} e^{-|z-z_i|/\lambda^{\sigma}} + \sum_l \operatorname{Re} \Delta_l^{\sigma} e^{-|z-z_l|/\lambda^{\sigma}} \right\}, \quad (3a)$$

$$\lambda^{\sigma} = T \left\{ \sum_{i \in T} \operatorname{Re} \Delta_i^{\sigma} + \sum_{l \in T} \operatorname{Re} \Delta_l^{\sigma} \right\}^{-1}, \quad (3b)$$

and

$$\operatorname{Re} \Delta_i^{\sigma} = \frac{1}{\lambda'} \langle \sigma | (1 + p_i \boldsymbol{\sigma} \cdot \mathbf{M}_i)^2 | \sigma \rangle, \quad (4a)$$

$$\operatorname{Re} \Delta_l^{\sigma} = \frac{a_0}{\lambda_l} \langle \sigma | (1 + p_l \boldsymbol{\sigma} \cdot \mathbf{M}_l)^2 | \sigma \rangle. \quad (4b)$$

Here n is the free electron density, e the electronic charge, m the electron mass, k_F the Fermi wave number, and T [= $2 \times (t_{\text{Co}} + t_{\text{Cu}})$] one period of the superlattice. The summation in Eq. (2) is over the two spin directions; z_i and z_l in Eq. (3a) represent the position of a Co/Cu interface and a lattice plane, respectively. The summations in Eq. (3b) are over interfaces and lattice planes within one superlattice period T . Equations (4a),(4b) contain the scattering matrix elements at the Co/Cu interface and in the bulk, respectively. \mathbf{M}_i and \mathbf{M}_l denote the magnetization at an interface and a lattice plane, respectively; p_i and p_l are the important fitting parameters representing the ratio of spin-dependent to spin-independent scattering at an interface or a lattice plane. These should not be confused with the ratios of spin-up over spin-down scattering, but they are of course related [$\alpha = \lambda_{\uparrow}/\lambda_{\downarrow} = (1+p)^2/(1-p)^2$]. The quantities λ' and λ_l are fitting parameters determining the magnitude of the scattering lengths due to interface and bulk scattering, respectively. The lattice plane distance is denoted by a_0 .

To calculate the MR we average Eq. (2) over the z coordinate for the situations of parallel and antiparallel alignments. For the prefactor $ne^2/\hbar k_F$ we used $2 \times 10^{15} (\Omega \text{ m}^2)^{-1}$, which is the mean value of Co and Cu in the free-electron model. We will only compare our low-temperature MR values with the quantum model, since

in Eq. (2) it is assumed that the two spin channels are independent, which may no longer be true at elevated temperatures, due to spin mixing.

In Fig. 8(a) we plot our experimental MR data as a function of the Cu spacer layer thickness at 4 K in the first two AF-coupling peaks. The top point of each peak now represents the MR value of a 100% antiparallel aligned sample, as determined from the analysis shown in Fig. 7. In this way, the theoretical expressions (2)–(4) can be used for comparison of these maxima. Since theory describes the case of complete antiparallel alignment, it only reproduces correctly the extrapolated MR values in the first and second AF-coupling peaks and not the oscillatory behavior (dashed line). The solid line in Fig. 8(a) is a calculation using the quantum model of MR with the parameters $p_i = 0.64$, $p_i^{\text{Co}} = 0.23$, $p_i^{\text{Cu}} = 0$ (as Cu is a nonferromagnetic metal), $\lambda_l^{\text{Co}} = 20 \text{ \AA}$, $\lambda_l^{\text{Cu}} = 250 \text{ \AA}$, and $\lambda' = 2.0$. Figure 8(b) depicts another set of MR data at 4 K, in which the Cu spacer layer thickness t_{Cu} was fixed at 20 \AA (second AF peak) and the magnetic layer thickness t_{Co} was varied. In that way, we are able to discriminate between interface and bulk-Co contributions

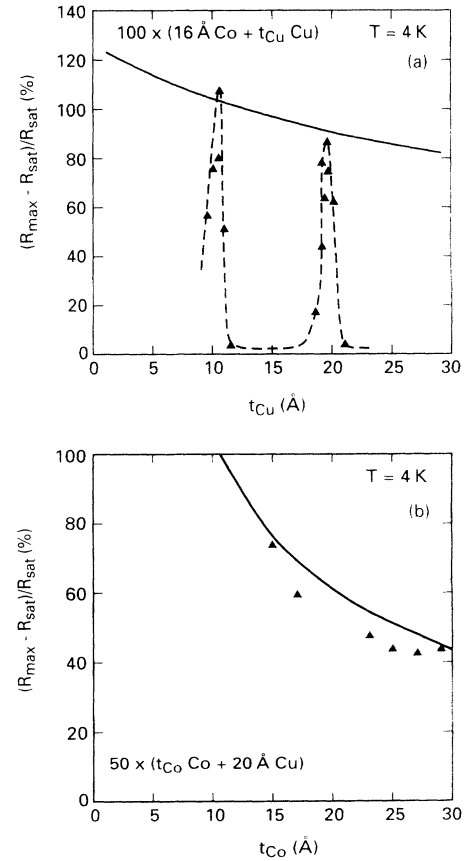


FIG. 8. (a) Dependence of the magnetoresistance on the Cu spacer layer thickness t_{Cu} at $T = 4 \text{ K}$. The solid line is calculated using the quantum model of Levy *et al.* (Ref. 12); the dashed curve is a guide to the eye. (b) Dependence of the magnetoresistance on the magnetic layer thickness t_{Co} at $T = 4 \text{ K}$. The solid line is a calculation with the quantum model. Fitting parameters are indicated in the text.

to the spin-dependent scattering. Since these multilayer samples correspond to the second AF maximum, they all show large AF-coupling fractions of 0.8–0.9. The data plotted in Fig. 8(b) are corrected for complete AF coupling, just as it was the case for the data in Fig. 8(a). Again, the solid line is a calculation using the quantum model of MR, with essentially the same parameters²⁷ as in the calculations of Fig. 8(a): $p_i = 0.64$, $p_i^{\text{Co}} = 0.23$, $p_i^{\text{Cu}} = 0$, $\lambda_i^{\text{Co}} = 16 \text{ \AA}$, $\lambda_i^{\text{Cu}} = 210 \text{ \AA}$, and $\lambda' = 2.0$.

Let us now discuss the significance of the various fitting parameters. It follows that reasonable fits that describe both the data in Figs. 8(a) and 8(b) simultaneously can only be obtained for $p_i = 0.64 \pm 0.02$ ($\alpha_i = 21 \pm 3$) and $p_i^{\text{Co}} = 0.23 \pm 0.03$ ($\alpha^{\text{Co}} = 2.6 \pm 0.3$). This value for the bulk asymmetry parameter in Co agrees well with the results of Zhang and Levy,²⁸ and also with those of Pratt *et al.*,²⁹ obtained from the analysis of MR measurements of several Co-based multilayer systems with the current perpendicular to the multilayer planes. Hence, it seems to be an intrinsic property of bulk Co. The Co/Cu-interface asymmetry parameter p_i (α_i), however, is rather large compared to the results of Pratt *et al.*²⁹ for sputtered Co/Cu(111) multilayers ($\alpha_i = 6.1 \pm 1.5$). Zhang and Levy²⁸ also find a considerably smaller value of $\alpha_i \simeq 10$. So this suggests that p_i (α_i) is more dependent on the exact microstructure, orientation, and deposition conditions. For our samples, the large value for α_i is mainly the origin of the large MR values in the first and second AF-coupling peak. The length λ_i^{Cu} is the dominant cause for the decrease in MR when going from the first to the second AF coupling peak [see Fig. 8(a)] and must be in the range $210 \text{ \AA} < \lambda_i^{\text{Cu}} < 250 \text{ \AA}$. This result agrees with the large values of λ_i^{Cu} reported in literature. The length λ_i^{Co} , on the other hand, is mainly responsible for the decrease of the MR with increasing t_{Co} [see Fig. 8(b)]; it is found to be within the range $16 \text{ \AA} < \lambda_i^{\text{Co}} < 20 \text{ \AA}$. The parameter λ' , determining the scattering length for interface scattering, can be varied between 1.8 and 2.2, without really worsening the fits. With these fitting parameters we obtain for the first and second AF-coupling peak ($t_{\text{Co}} = 16 \text{ \AA}$) typical multilayer resistivities ρ_{AF} of 77 and 61 $\mu\Omega \text{ cm}$, respectively. These are about a factor of 3 larger than experimentally determined resistivities, which may be due to the value of the prefactor in Eq.

(2), which was taken from the free-electron model. The same discrepancy was also found in the case of Fe/Cr multilayers.^{12,13} Our main conclusion is that large spin-dependent interface scattering is absolutely necessary to explain the giant MR effect in Co/Cu, and that the contribution from the spin-dependent bulk scattering is small. This is in accordance with the findings of Parkin, that the giant MR effect is determined by the character of the ferromagnetic/nonmagnetic interfaces.³⁰

V. SUMMARY

We have grown sputtered Co/Cu(100) multilayers on Cu buffer layers with different thicknesses. We found that the measured MR value for the first AF-coupling peak is very sensitive to the thickness of the Cu buffer layer, whereas it is not for the second AF peak. This is described to the relative importance of interface roughness in combination with the width of the AF-coupling maxima. Furthermore, we have observed a linear relationship between the actual measured MR ratio and the fraction of AF coupling, with maximum MR values at room temperature for the first and second AF peak of 65% and 46%, respectively (108% and 87%, respectively, at 4 K). These values were interpreted with the quantum model of magnetoresistance of Levy, Zhang, and Fert¹² from which we found evidence that spin-dependent scattering at the Co/Cu interfaces is the main cause for the giant MR effect.

ACKNOWLEDGMENTS

Part of this research was supported by the European Community Science Project ESPRIT3: Basic Research, "Study of Magnetic Multilayers for Magnetoresistive Sensors" (SmMmS). The authors would like to thank H.T. Munsters for the sample preparation, H. Nulens, M. van Opstal, and T. Schudelaro for their experimental assistance, and R. Coehoorn, A.M. Duif, H. van Houten, and M.T. Johnson for stimulating discussions.

¹ *Proceedings of the International Symposium on Magnetic Ultrathin Films, Multilayers and Surfaces, 7–10 September 1992, Lyon* [J. Magn. Magn. Mater. **121**, 1 (1993)].

² *Magnetic Ultrathin Films: Multilayers and Surfaces/Interfaces and Characterization*, edited by B.T. Jonker, S.A. Chambers, R.F.C. Farrow, C. Chappert, R. Clarke, W.J.M. de Jonge, T. Egami, P. Grünberg, K.M. Krishnan, E.E. Marinero, C. Rau, and S. Tsunashima, MRS Symposia Proceedings No. 313 (Materials Research Society, Pittsburgh, 1993).

³ *Proceedings of the MMM Conference, 15–19 November 1993, Minneapolis* [J. Appl. Phys. **75** (10), Pt. II (1994)].

⁴ R.E. Camley and J. Barnaś, Phys. Rev. Lett. **63**, 664

(1989).

⁵ A. Barthélémy and A. Fert, Phys. Rev. B **43**, 13124 (1991).

⁶ B.L. Johnson and R.E. Camley, Phys. Rev. B **44**, 9997 (1991).

⁷ B. Dieny, Europhys. Lett. **17**, 261 (1992); J. Phys. Condens. Matter **4**, 8009 (1992).

⁸ Th.G.S.M. Rijks, R. Coehoorn, and W.J.M. de Jonge, in *Magnetic Ultrathin Films: Multilayers and Surfaces/Interfaces and Characterization* (Ref. 2), p. 283.

⁹ L.M. Falicov and R.Q. Hood, J. Magn. Magn. Mater. **121**, 362 (1993).

¹⁰ J.L. Duvail, A. Fert, L.G. Pereira, and D.K. Lottis, J. Appl. Phys. **75**, 7070 (1994).

- ¹¹ B. Dieny, V.S. Speriosu, J.P. Nozières, B.A. Gurney, A. Vedyayev, and N. Ryzhanova, in *Structure and Magnetism in Systems of Reduced Dimension*, Vol. 309 of *NATO Advanced Study Institute, Series B: Physics* edited by R.F.C. Farrow *et al.* (Plenum, New York, 1993), p. 279.
- ¹² P.M. Levy, S. Zhang, and A. Fert, *Phys. Rev. Lett.* **65**, 1643 (1990); S. Zhang, P.M. Levy, and A. Fert, *Phys. Rev. B* **45**, 8689 (1992).
- ¹³ M.A.M. Gijs and M. Okada, *Phys. Rev. B* **46**, 2908 (1992); *J. Magn. Magn. Mater.* **113**, 105 (1992).
- ¹⁴ R. Coehoorn, A. De Veirman, and J.P.W.B. Duchateau, *J. Magn. Magn. Mater.* **121**, 266 (1993); R. Coehoorn and J.P.W.B. Duchateau, *ibid.* **126**, 390 (1993).
- ¹⁵ R. Coehoorn, M.T. Johnson, W. Folkerts, S.T. Purcell, N.W.E. McGee, A. de Veirman, and P.J.H. Bloemen, in *Structure and Magnetism in Systems of Reduced Dimension* (Ref. 11), p. 295.
- ¹⁶ D.H. Mosca, F. Petroff, A. Fert, P.A. Schroeder, W.P. Pratt, Jr., and R. Loloe, *J. Magn. Magn. Mater.* **94**, L1 (1991).
- ¹⁷ M.T. Johnson, S.T. Purcell, N.W.E. McGee, R. Coehoorn, J. aan de Stegge, and W. Hoving, *Phys. Rev. Lett.* **68**, 2688 (1992).
- ¹⁸ P.J.H. Bloemen, R. van Dalen, W.J.M. de Jonge, M.T. Johnson, and J. aan de Stegge, *J. Appl. Phys.* **73**, 5972 (1993).
- ¹⁹ F. Giron, P. Boher, Ph. Houdy, P. Beauvillain, K. Le Dang, and P. Veillet, *J. Magn. Magn. Mater.* **121**, 318 (1993).
- ²⁰ E.E. Fullerton, D.M. Kelly, J. Guimpel, I.K. Schuller, and Y. Bruynseraede, *Phys. Rev. Lett.* **68**, 859 (1992); E.E. Fullerton, M.J. Conover, J.E. Mattson, C.H. Sowers, and S.D. Bader, *Phys. Rev. B* **48**, 15755 (1993).
- ²¹ R.J. Highmore, J.E. Evetts, and R.E. Somekh, *J. Magn. Magn. Mater.* **123**, L13 (1993).
- ²² G. Rupp and K. Schuster, *J. Magn. Magn. Mater.* **121**, 416 (1993); H.A.M. van den Berg and G. Rupp (unpublished).
- ²³ B. Dieny, J.P. Gavigan, and J.P. Rebouillat, *J. Phys. Condens. Matter* **2**, 159 (1990); B. Dieny and J.P. Gavigan, *ibid.* **2**, 187 (1990).
- ²⁴ W. Folkerts, *J. Magn. Magn. Mater.* **94**, 302 (1991).
- ²⁵ R. Coehoorn (private communication).
- ²⁶ S.S.P. Parkin, R. Bhadra, and K.P. Roche, *Phys. Rev. Lett.* **66**, 2152 (1991); S.S.P. Parkin, Z.G. Li, and D.J. Smith, *Appl. Phys. Lett.* **58**, 2710 (1991).
- ²⁷ The small difference in the parameters λ_i^{Co} and λ_i^{Cu} may be due to the different number of repetitions, n , used in the two data series [$n = 100$ for the series in Fig. 8(a) and $n = 50$ for the series in Fig. 8(b)], which influences the relative contributions of the Cu buffer layer to the MR.
- ²⁸ S. Zhang and P.M. Levy, *Phys. Rev. B* **47**, 6776 (1993).
- ²⁹ W.P. Pratt, Jr., S.-F. Lee, Q. Yang, P. Holody, R. Loloe, P.A. Schroeder, and J. Bass, *J. Appl. Phys.* **73**, 5326 (1993); P.A. Schroeder, J. Bass, P. Holody, S.-F. Lee, R. Loloe, W.P. Pratt Jr., and Q. Yang, in *Magnetic Ultrathin Films: Multilayers and Surfaces/Interfaces and Characterization* (Ref. 2), p. 47.
- ³⁰ S.S.P. Parkin, *Phys. Rev. Lett.* **71**, 1641 (1993).